Monolithic Integration of III-V Photodiodes and Emitters on Silicon

C. Oliver Martinez[2], M. Scherrer[2], S. Iadanza[1,3], P. Wen[2], P. Tiwari[1,2], M. Sousa[2], B. Gotsmann[2], H. Schmid[2] and K. E. Moselund[1,3]

(1) Paul Scherrer Institut, Laboratory of Nano and Quantum Technologies; 5232 Villigen PSI Schweiz, kirsten.moselund@psi.ch
(2) IBM Research Europe Zurich, 8803 Rüschlikon, Switzerland cri@zurich.ibm.com
(3) EPFL, Integrated Nanoscale Photonics and Optoelectronics Laboratory, 1015 Lausanne, Switzerland.

Abstract *Waveguide coupled III-V heterostructure photodetectors are fabricated by template-assisted selective epitaxy. The devices show responsivities up to 0.2 A/W and 3dB frequencies exceeding 50 GHz. The TASE method allows for a seamless integration of III-Vs with Si features and we also demonstrate hybrid III-V/Si photonic crystal emitters.*

Introduction

Silicon electronic integrated circuits (ICs) are facing a bottleneck due to the resistive interconnect. To address this issue, researchers have been working to combine electronics and photonics on a silicon chip, to use electronics for computation, while photonics can provide low loss signal transmission and greater bandwidth(1).

SiGe or pure Ge represents the state of the art in terms of on-chip integrated photodetectors(2–4). SiGe compounds are considered CMOS compatible as they are also used in conventional high-performance electronics. Therefore, their integration for photonics is straightforward. High-speeds (beyond 50 GHz) have been achieved. Ge-based devices are particularly suited for on-chip applications in the O-band around 1300nm as their efficiencies tend to drop off in the c-band beyond 1500 nm. However, the indirect bandgap of SiGe make them unsuited for light emission. III-Vs provide widely tunable direct band-gaps, the ability to tailor a broad range of heterostructures and can be extended further towards the NIR by changing the composition (5,6). These properties also render them attractive for light detection, but their integration on silicon is more challenging.

One promising approach is to bond a III-V stack including quantum wells on top of a silicon wafer with pre-fabricated waveguides and passives (7,8). Today's state-of-the-art high-performance integrated photonic components tend to be orders of magnitude larger measuring 100s of micrometers. To reduce the RC time constant and power consumption, research efforts have been focused on the development of scaled hybrid III-V/Si nanophotonic devices, including nanowire photodetectors and light sources.

Waveguide couple photodetectors

In this talk we will discuss on work, waveguide coupled devices with grating couplers centered at 1320 nm were studied using two different device architectures based on either a straight or a T-shape architecture. Double heterostructures (n-InP/i-InGaAs/p-InP/p-InGaAs) were implemented to improve carrier confinement(9).

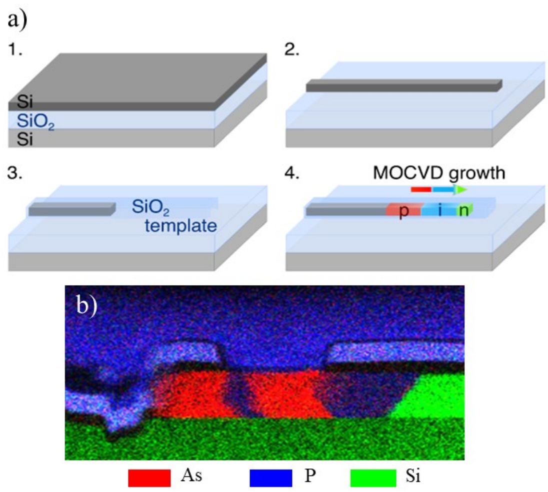

Figure 1 a) Schematic of the TASEprocess flow: 1) starting point is an SOI wafer with ~220 nm Si thickness. 2) All desired features – Si passives (waveguides, grating couplers, mirrors as well as future III-V areas are etched in a single lithographic step. 3) The etched structures are coved by template oxide, an opening is made and the Si to be replaced by III-V is etched away. 4) III-V is regrown within the template oxide. B) EDS overview map for SEM cross-section of a regrown n-InP/i-InGaAS/p-InP/p-InGaAs heterostructure (the bluish colour on top of the device is from the Au and Pt metallization whose signature is close to phosphorous).

The devices are fabricated by template assisted selective epitaxy (TASE)(10,11) as illustrated in Figure 1. Features of devices and passives are defined by e-beam lithography and dry etching of the 220nm thick top silicon layer of

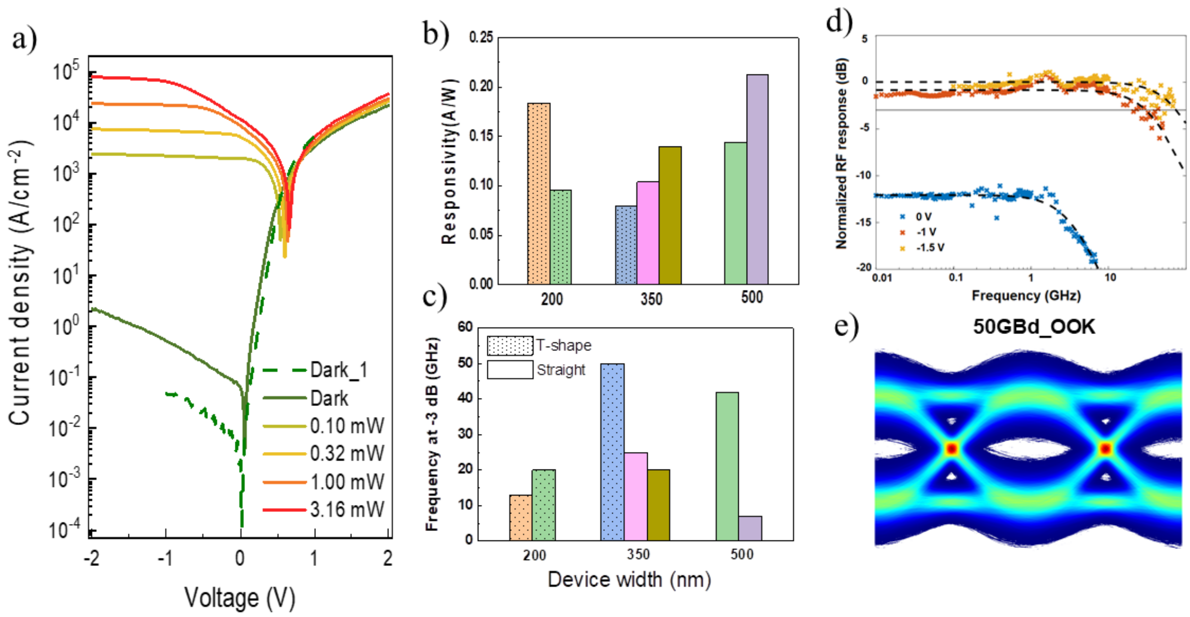

Figure 2 Characteristics of the pin photodetectors. A) I-V curves of a t-shaped device without light (dark green) and with 1320 nm waveguide coupled laser power varying from 0.1 mW to 3.16 mW. b) Responsivity (at –2 V) dependence on device architecture and device width. C) f3dB dependence on device architecture and device width. d) Radio frequency (RF) signal response dependence on modulation frequency of the input signal. e) 50GBd OOK eye diagram.

a SOI wafer. Subsequently, the silicon features are embedded in a uniform SiO_2 layer and those regions to be replaced by III-V active material is selectively etched back to form a hollow oxide template. The III-V heterojunction profile is grown within the template by MOCVD and Ni-Au metal contacts are implemented by e-beam lithography and lift-off. Other groups have taken up the TASE epitaxial technique as well for electronics (12,13) as well as photonic applications (14).

In this work which is based upon (9,15), two different device architectures were explored: the straight device and the T-shape device. The straight structure is easier from a conceptual point of view but the drawback is that contacts will inevitably need to be in the path of the optical mode. The T-shape structure does not require contacts to be placed on top of the waveguide, but the coupling efficiency across the thin gap is unknown and might lead to back-reflections in the silicon waveguide.

Different detector performance metrics are illustrated in Figure 2. Relatively low dark currents are observed along with responsivities up to 0.2 A/W and 3dB frequencies exceeding 50 GHz. Detector performance was also evaluated under various signal encoding schemes, and data reception at 50 GBd on-off keying (OOK) was observed.

LED emission

In forward bias, the device functions as an LED with the undoped InGaAs region as the active emitter, but the grating couplers are not optimized for the emission wavelength of 1550 nm. Thus, emission measurements were done with a free-space coupled optical setup in reflection mode. As illustrated in Figure 3, electroluminescence measurements were performed at temperatures ranging from 80 K to 300 K under continuous wave operation. The EL peak shifts with increasing bias, party because of a strong temperature dependence of the diode threshold voltage. The injection-current dependent blueshift of the EL peak is likely due to the band filling effect of the carrier injection in the active region.

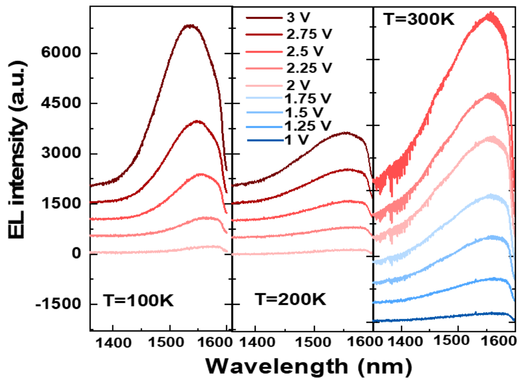

Figure 3 Electroluminescence (EL) spectra of a 350 nm wide T-shape device (T3) under CW operation, measured at 100 K, 200 K and 300 K, from (9).

Hybrid III-V/Si resonant emitters

Whereas the platform is less mature compared to waferbonding, the TASE integration approach ultimately allows for a more seamless integration with Si features, and therefore more scaled devices.

This is perfectly illustrated in our work on hybrid III-V/Si photonic crystal structures where the TASE method allows us to replace select parts of a silicon lattice with active material, perfectly aligned at the nm-scale. Using this method we have demonstrated photonic crystal resonant emitters operating over the entire telecom bandwidth(16,17), see the illustration of this concept in Figure 4.

The spectral profile of emission and detection is compared in Figure 5, for our first batch of devices which were too thin (60 nm) to allow for mode propagation (18,19).

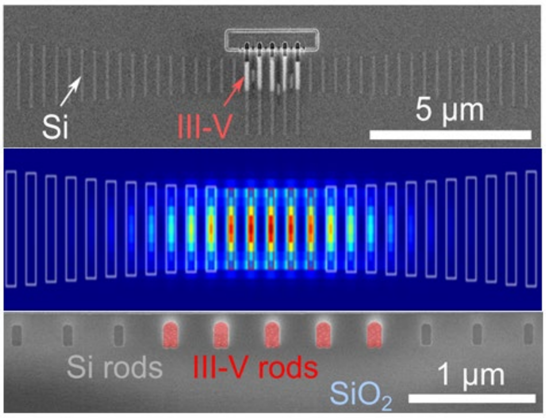

Figure 4 Illustration of the concept of hybrid III-V Si photonic crytsla lasers. Using TASE the central rods are replaced by active III-V gain material whereas the mirrors are kept as transparent silicon. There is an epitaxial connection with between the Si layer and the regrown III-V material (16)

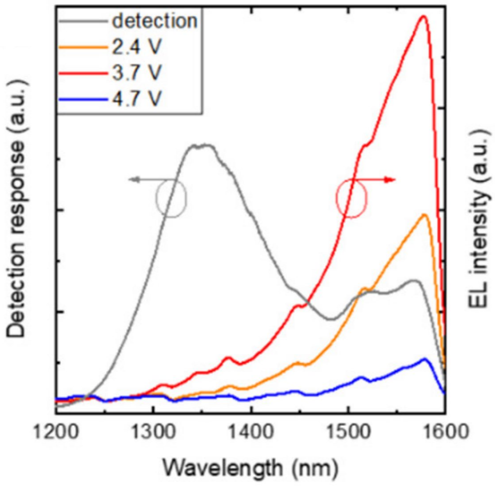

Figure 5 Comparison of the detection response of the first generation phtoodetctors (18) and corresponding LED emission from the same InGaAs structures**.** Figure adapted from (17).

Perhaps the versatility of the approach is even better illustrated by recent work on topological photonic crystal designs(20), where III-V and Si rods are perfectly interlaced to provide distributed gain in a topological photonic crystal lattice.

Conclusions

To summarize, our work demonstrated the integration of III-V heterostructure photodiodes on Si with submicron dimensions. The devices emitted light centered at 1550 nm and showed a blueshift with increasing bias. In photodetection mode, the devices showed a low dark current and high responsivity. A detection bandwidth exceeding 70 GHz was achieved with grating couplers centered around 1320 nm, enabling data transmission at 50 GBd with OOK and 4PAM. The integration approach via TASE represents a new paradigm for densely integrated hybrid III-V/Si photonics schemes and can be extended to an all-optical high-speed link on Si without the need for evanescent coupling.

Acknowledgements

We acknowledge financial support from H2020 ERC StG PLASMIC no 678567 and H2020 MSCA IF project DATENE no 844541, as well as SNF projects LIVE-EDC grant no 200021M_192028 and Korean-Swiss joint program, SNF grant No. 188173

We thank the Cleanroom Operations Team of the Binnig and Rohrer Nanotechnology Center (BRNC) for their help and support.

References

1. Miller DAB. Attojoule Optoelectronics for Low-Energy Information Processing and Communications. J Light Technol. 2017;35(3).
2. Lischke S, Peczek A, Korndorfer F, Mai C, Haisch H, Koenigsmann M, et al. Ge photodiode with -3 dB OE bandwidth of 110 GHz for PIC and ePIC platforms. In: Technical Digest - International Electron Devices Meeting, IEDM. 2020.
3. Lischke S, Peczek A, Morgan JS, Sun K, Steckler D, Yamamoto Y, et al. Ultra-fast germanium photodiode with 3-dB bandwidth of 265 GHz. Nat Photonics. 2021;15(12).
4. Hu X, Wu D, Chen D, Wang L, Xiao X, Yu S. 180 Gbit/s Si 3 N 4 -waveguide coupled germanium photodetector with improved quantum efficiency . Opt Lett. 2021;46(24).
5. Han Y, Park H, Bowers J, Lau KM. Recent advances in light sources on silicon. Adv Opt Photonics. 2022 Sep 30;14(3):404.
6. Kim H, Farrell AC, Senanayake P, Lee WJ, Huffaker DL. Monolithically Integrated InGaAs Nanowires on 3D Structured Silicon-on-Insulator as a New Platform for Full Optical Links. Nano Lett. 2016;16(3).
7. Xiang C, Guo J, Jin W, Wu L, Peters J, Xie W, et al. High-performance lasers for fully integrated silicon nitride photonics. Nat Commun. 2021;12(1).
8. Baumgartner Y, Caimi D, Sousa M, Hopstaken M, Salamin Y, Baeuerle B, et al. High-speed CMOS-compatible III-V on Si membrane photodetectors. Opt Express. 2021;29(1).

9. Wen P, Tiwari P, Mauthe S, Schmid H, Sousa M, Scherrer M, et al. Waveguide coupled III-V photodiodes monolithically integrated on Si. Nat Commun. 2022;13(1).

10. Schmid H, Cutaia D, Gooth J, Wirths S, Bologna N, Moselund KE, et al. Monolithic integration of multiple III-V semiconductors on Si for MOSFETs and TFETs. In: Technical Digest - International Electron Devices Meeting, IEDM. 2017.

11. Borg M, Gignac L, Bruley J, Malmgren A, Sant S, Convertino C, et al. Facet-selective group-III incorporation in InGaAs template assisted selective epitaxy. Nanotechnology. 2019;30(8).

12. Šuran Brunelli ST, Goswami A, Markman B, Tseng HY, Rodwell M, Palmstrøm C, et al. Horizontal heterojunction integration via template-Assisted selective epitaxy. Cryst Growth Des. 2019;19(12).

13. Goswami A, Markman B, Brunelli STŠ, Chatterjee S, Klamkin J, Rodwell M, et al. Confined lateral epitaxial overgrowth of InGaAs: Mechanisms and electronic properties. J Appl Phys. 2021;130(8).

14. Yan Z, Han Y, Lin L, Xue Y, Ma C, Ng WK, et al. A monolithic InP/SOI platform for integrated photonics. Light Sci Appl. 2021;10(1).

15. Tiwari P, Wen P, Mauthe S, Baumann M, Bitachon BI, Schmid H, et al. Butt-Coupled III-V Photodetector Monolithically Integrated on SOI with data reception at 50 Gbps OOK. In: 2021 Optical Fiber Communications Conference and Exhibition, OFC 2021 - Proceedings. 2021.

16. Mauthe S, Tiwari P, Scherrer M, Caimi D, Sousa M, Schmid H, et al. Hybrid III-V Silicon Photonic Crystal Cavity Emitting at Telecom Wavelengths. Nano Lett. 2020;20(12).

17. Scherrer M, Triviño NV, Mauthe S, Tiwari P, Schmid H, Moselund KE. In-plane monolithic integration of scaled iii-v photonic devices. Vol. 11, Applied Sciences (Switzerland). 2021.

18. Mauthe S, Baumgartner Y, Sousa M, Ding Q, Rossell MD, Schenk A, et al. High-speed III-V nanowire photodetector monolithically integrated on Si. Nat Commun. 2020;11(1).

19. Mauthe S, Baumgartner Y, Sant S, Ding Q, Sousa M, Czornomaz L, et al. Ultra-thin III-V photodetectors epitaxially integrated on Si with bandwidth exceeding 25 GHz. In: Optics InfoBase Conference Papers. 2020.

20. Scherrer M, Kim S, Choi HJ, Schmid H, Lee C-W, Moselund K. Single-mode emission from a topological lattice with distributed gain and dielectric medium. Ofc. 2022;(c).